Article:
Soltanahmadi, S, Morina, A, Eijk, MCPV et al. (2017) Experimental Observation of Zinc Dialkyl DithioPhosphate (ZDDP)-Induced Iron Sulphide Formation. Applied Surface Science, 414. pp. 41-51. ISSN: 0169-4332

https://doi.org/10.1016/j.apsusc.2017.04.023

Title: Experimental Observation of Zinc Dialkyl DithioPhosphate (ZDDP)-Induced Iron Sulphide Formation

Author: Siavash Soltanahmadi Ardian Morina Marcel C. P. van Eijk Ileana Nedelcu Anne Neville

PII: S0169-4332(17)31028-0
DOI: http://dx.doi.org/doi:10.1016/j.apsusc.2017.04.023
Reference: APSUSC 35696

To appear in: *APSUSC*

Received date: 22-11-2016
Revised date: 1-4-2017
Accepted date: 4-4-2017

Please cite this article as: <doi>http://dx.doi.org/10.1016/j.apsusc.2017.04.023</doi>

Experimental Observation of Zinc Dialkyl DithioPhosphate (ZDDP)-Induced Iron Sulphide Formation

Siavash Soltanahmadi[a*], Ardian Morina[a], Marcel C. P. van Eijk[b], Ileana Nedelcu[b], and Anne Neville[a]

*s.soltanahmadi@leeds.ac.uk

[a]Institute of Functional Surfaces, School of Mechanical Engineering, University of Leeds, LS2 9JT, UK

[b]SKF Engineering and Research Centre, 3430 DT Nieuwegein, The Netherlands

Abstract

Zinc Dialkyl DithioPhosphate (ZDDP) as a well-known anti-wear additive enhances the performance of the lubricant beyond its wear-protection action, through its anti-oxidant and Extreme Pressure (EP) functionality. In spite of over thirty years of research attempting to reveal the mechanism of action of ZDDP, there are still some uncertainties around the exact mechanisms of its action. This is especially the case with the role of sulphide layer formed in the tribofilm and its impact on surface fatigue. Although iron sulphide on the substrate is hypothesised in literature to form as a separate layer, there has been no concrete experimental observation on the distribution of the iron sulphide as a dispersed precipitate, distinct layer at the steel substrate or both. It remains to be clarified whether the iron sulphide layer homogeneously covers the surface or locally forms at the surface. In the current study a cross section of the specimen after experiment was prepared and has been investigated with Transmission Electron Microscopy (TEM) and Energy-Dispersive X-ray (EDX) elemental analysis. A 5-10 nm iron sulphide layer is visualised on the interface as a separate layer underneath the phosphate layer with an altered distribution of tribofilm elements near the crack site. The iron sulphide interface layer is more visible near the crack site where the concentration of the sulphur is enhanced. Also, ZDDP elements were clearly detected inside the crack with a varied relative concentration from the crack-mouth to the crack-tip. Sulphur is present inside the crack to a higher extent than in the bulk of the tribofilm.

1 Introduction

Anti-wear (AW)and EP additives, Sulphur-Phosphorus (S-P) compounds are essential in highly loaded-gears and bearings in order to reduce scuffing and mitigate abrasive and adhesive wear[1, 2]. AW and EP additives can improve fatigue life [2, 3] at low concentrations [3] especially at large contact pressures[4]. In contrast, there are reports

showing S-P containing additives can be detrimental to fatigue life of the bearings[3, 5-8]. The reduced rolling contact fatigue life has been attributed to the chemical attack of the reactive additives which can induce crack or pit nucleation[3, 5, 6, 9].

Furthermore, AW additives have been strongly shown to enhance the incidences of micropitting[10-12]. On the other hand, O'Connor [13] showed that assigning EP or AW additives as detrimental or beneficial additive as a general statement can be misleading. Thus the literature suggests that the impact of the additives on micropitting wear depends on the concentration, chemical structure of the additives and application. Therefore, detailed tribochemical studies of each individual additive and their interactions are required. The enhancing effect of ZDDP on micropitting was investigated mainly taking the mechanical and tribological aspects of micropitting into account [14, 15] and the tribochemical effect of ZDDP in severe micropitting wear has not been completely elucidated in rolling-sliding conditions.

1.1 The role and chemical nature of sulphides in the ZDDP tribofilm

ZDDP as an AW additive is particularly believed to protect the surface from wear through forming an adherent (poly) phosphate layer on the steel substrate. ZDDP also has an insubstantial EP activity in comparison to some other metal dialkyl dithiophosphates [16]. Thermal degradation of ZDDP can convert the most of the sulphur in ZDDP to oil-soluble organic sulphides and disulphides which can act as EP additives [17]. Organic sulphides are widely used EP additives which at high temperatures induced by high local pressure (shear and stress) are inferred to protect surfaces through surface passivation [18] i.e. forming iron-sulphur compound [19].

The sulphide contribution to the bulk of the ZDDP tribofilm is expected to be mainly zinc sulphide[20, 21]. Cation exchange from zinc sulphide to form iron sulphide is not thermodynamically favourable [21] which implies that iron sulphide formation can take place through reaction of organic sulphide species with the steel surfaces as also suggested by Martin [20, 22]. The iron sulphide can be formed in the event of removal of the (poly)phosphates followed by acid-base reactions of the organic sulphides with nascent surface [20]. The nature of the ZDDP-derived iron sulphide can be FeS[20, 23, 24], FeS_2[20], Fe_7S_6[25] or Fe_7S_8[26]. However, in the sulphidation reaction of nascent iron surface, FeS is the most probable compound [27] especially under severe contacts [19]. As an interfacial

layer, iron sulphide in combination with iron oxide formation is suggested using Auger spectroscopy[28, 29].

1.2 Current understanding of the iron sulphide formation from ZDDP molecule

As far as ZDDP is concerned, iron sulphide formation has been observed on the wear particles as nanprecipitates[20, 26]. Hallouis et al.[26] suggested Fe_7S_8 as the composition of the iron sulphide nanoprecipitates. Minfray et al. [30] used *in-situ* Auger spectroscopy and rubbed a pin having iron-oxide on the surface against a pre-formed ZDDP tribofilm under a severe condition where lubricant was absent and observed formation of iron sulphide as the main compound in the reaction layer on the pin.

Bell et al. [31] analysed tribofilm generated from ZDTP-containing mineral oil at 175°C on a pure iron foil and showed that S^- peak seats at a deeper level than PO_2^- and O^- peaks in dynamic secondary ion mass profile [31]. Employing X-ray Photoelectron Spectroscopy (XPS), they also observed increased contribution of oxide and sulphide peaks in iron signal through the tribofilm depth [31]. Accordingly, they suggested an iron sulphide and/or oxide on the substrate as shown in **Figure 1**(a).

Smith et al. [32] observed patches having Zn, Fe and S where P was not detected and discerned the existence of Zn, S and oxygen signals below phosphorous signal in XPS depth spectra [32]. Thus they suggested presence of a dense iron/zinc sulphide/oxide on the steel substrate as a distinct layer under phosphate layer (see **Figure 1**(b)). The three layer structure was then disputed by Martin[22]. Martin[22] suggested a two layer structure of ZDDP tribofilm composed of a 10nm-thin long chain poly(thio) phosphate at top and mixed Fe/ Zn short chain (poly)phosphate in bulk with metal sulphide precipitates embedded in its structure as illustrated in **Figure 1**(c). Martin et al. [20, 22] postulated a localised iron sulphide formation only in very severe conditions as presented in Figure 1(d). Spikes [17] in his review paper depicted the structure of the ZDDP tribofilm as shown in **Figure 1**(e) having an iron/zinc sulphide at the interface of substrate and phosphate glass.

XANES reports mainly rule out the existence of iron sulphide [23, 33-37] in a fully developed ZDDP tribofilm and specify formation of ZnS except few reports suggesting contribution of the iron sulphide together with zinc sulphide and Fe/Zn sulphate to the tribofilm throughout its depth as presented in **Figure 1** (f). However, excluding iron sulphide as part of the tribofilm could be due to the fact that a minor contribution of dispersed iron

sulphide or a very thin interfacial iron sulphide film is below the sensitivity of XANES Fluorescence Yield (FY) mode of detection on S L-edge [21, 33].

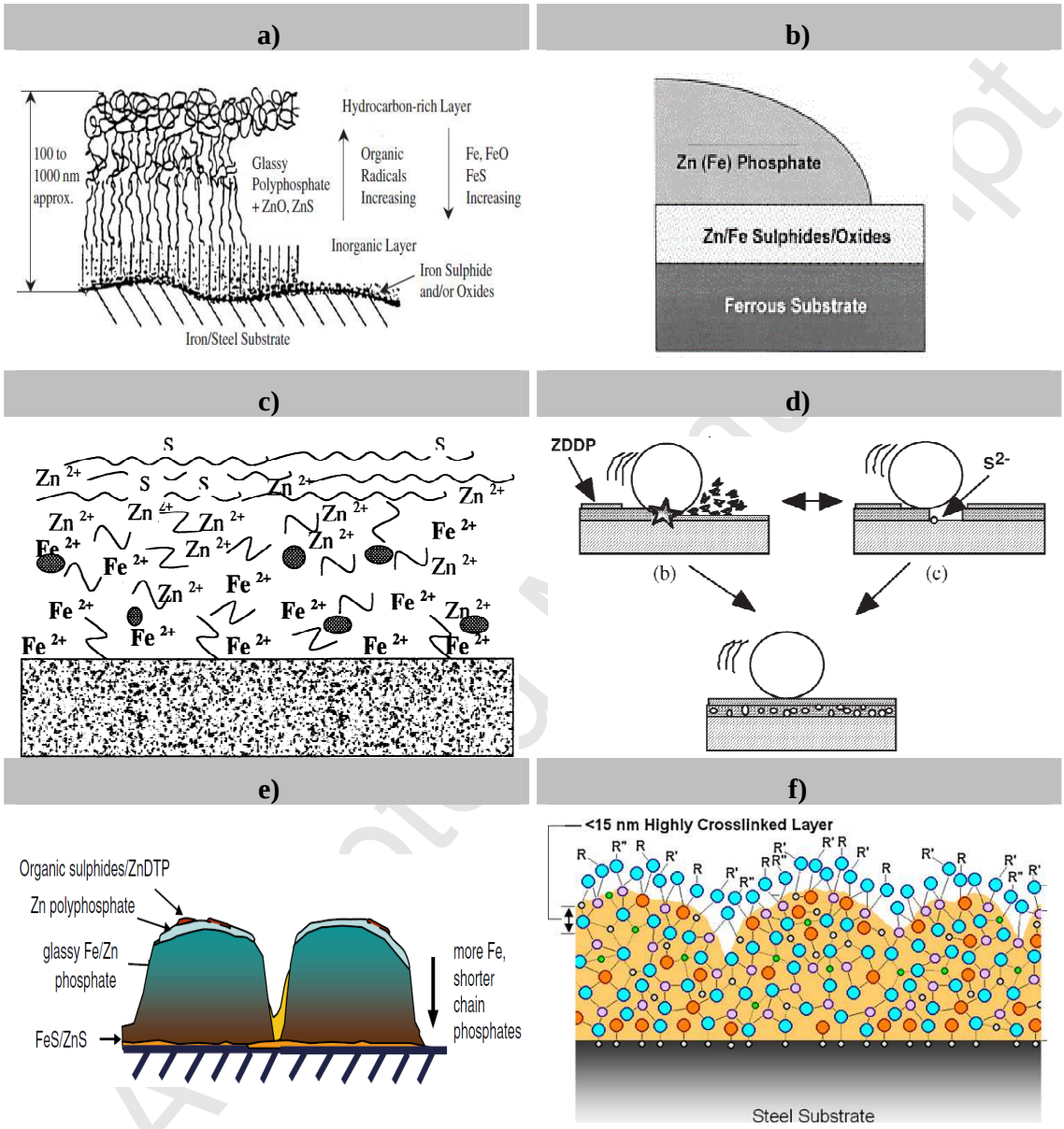

Figure 1. Schematic illustrations of ZDDP tribofilm structure suggested by a) Bell et al.[31] b) Smith et al.[32] c) Martin et al. [22]d) Martin[20] e) Spikes[17] f) Kim et al.[38] (WC ball on steel cylinder under EP contact)

A confirmation to this fact can be perceived in Zhang et al. [23] report in which a minor contribution of iron sulphide is detected after 10 s of rubbing in Total Electron Yield (TEY) S K-edge mode despite the fact that ZnS was dominant at this stage and in the further rubbing to form a thick film. In XANES and XPS analyses, collected signals are influenced by an

averaging effect over the analysed area and sampling depth. Accordingly, observation of the lateral and localised chemical distribution of compounds and elements throughout the tribofilm-depth and near the surface pits and cracks may not be achieved through these techniques.

Therefore, as a result of numerus studies using a variety of analytical methods, iron sulphide formation as part of a ZDDP tribofilm has been confirmed to form under certain conditions. However, some uncertainties still remain including whether iron sulphide exists as a dispersed precipitate, as a distinct layer at the substrate or both. Also, if it exists as a layer there are still questions around the uniformity of the layer. In addition, whether the iron sulphide layer exists alone [30, 39], in combination with iron oxide [29, 31] or zinc sulphide at the substrate surface has not been confirmed. Thus, further studies are required to determine whether iron sulphide as an interface layer entirely covers the surface or forms as a localised area.

In order to answer part of the mentioned uncertainties, in the current study a modified MicroPitting Rig (MPR) was used to generate ZDDP-derived tribofilms on a steel surface under a severe boundary lubrication regime followed by Focused Ion Beam (FIB) sectioning of the surface close to a micropit in order to observe the tribofilm distribution on the nanometer scale. The FIB cross section has been investigated with TEM-EDX elemental analysis to confirm the elements throughout the tribofilm cross section. The surface and reaction layer on the surface are investigated using Scanning Electron Microscopy (SEM) and XPS surface analytical technique.

2 Test setup to induce surface fatigue features

A modified PCS Instrument MPR tester which is schematically represented in **Table 1** is used to induce wear and surface fatigue and to generate ZDDP tribofilms on the steel surfaces. The inspected surface is the wear scar of a spherical roller. The roller (12 mm in diameter) was circumferentially polished to the roughness value of R_q= 50 ± 5 nm. The roller is located in the middle and undergoes cyclic load applied by three larger and equal-diameter counter bodies.

The rings are inner rings of cylindrical roller bearing (designation NU209) which are ground-finished transverse to the rolling/sliding direction with the roughness of R_q=500 ± 50 nm. Both the roller and rings were made of AISI 52100 steel. The measured macro hardness

number of the roller and rings is 785 (HV) and 745 (HV), respectively. The experimental conditions in the present work are indicated in **Table 1**.

Table 1. MPR rig illustration and test parameters

Specimens	Roller: 52100 steel, R_q: 50 nm HV: 785 Rings: 52100 steel, R_q: 500nm, HV: 745
Lubricant : Poly-Alpha-Olefin (PAO) + ZDDP	Phosphorous concentration: 0.08 Wt% kinematic viscosity (υ): 4 cSt @100°C
P_{max}	1.5 GPa
Temperature	90°C
Load cycles (on roller)	1×10^6
Slide-to-roll ratio (%)	2
Entrainment speed	1 m/s

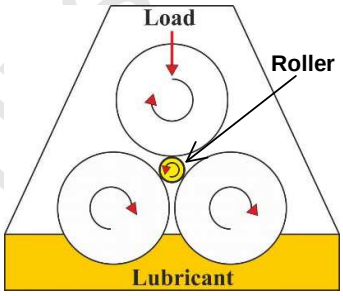

Schematic illustration of the tribometer

3 Analysis techniques

3.1 Scanning electron microscopy

A Zeiss Supra 55 SEM is utilised to capture images from the wear scar. Employing low acceleration voltage (5KV), images of the roller surface were obtained in Secondary Electron (SE) mode. Images were acquired following two different washing procedures. At first, images were taken from surface following three minutes of ultrasonic cleaning in a mild solvent (n-heptane) in order to remove the residual oil from surface. The solvent-removable reaction layer (which we will call it tribofilm henceforth) and the residual oil on the specimen surface were then removed thoroughly from the surface by wiping the specimen's surface using tissue and acetone followed by ultrasonic cleaning in acetone for thirty minutes and the images are acquired to inspect the surface after the tribofilm removal.

3.2 Chemical investigation of the tribofilm in micro-scale: XPS

XPS surface analysis has been carried out employing a PHI 5000 Versa Probe™ spectrometer (Ulvac-PHI Inc, Chanhassen, MN, USA) which uses a monochromatic Al Kα

X-ray source (1486.6 eV). The specimens have been ultrasonically cleaned in n-heptane for three minutes prior to XPS spectra acquisition in order to eliminate the residual oil from the surface.

Detailed spectra from the tribofilm are collected using a beam size of 100 µm in a fixed analysed transmission mode. The energy step size of 0.05 eV has been set for the oxygen, iron, phosphorous, and sulphur acquisition and 0.1 for carbon and zinc (2p). The residual chamber pressure was always lower than 5×10^{-7} Pa during spectra acquisition.

The detailed XPS spectra were fitted using CASAXPS software (version 2.3.16, Casa Software Ltd, UK) with Gaussian–Lorentzian curves after subtracting a Shirley background. Charge correction of the specimens has been performed by referring the aliphatic carbon binding energy to 285.0 eV. The fitting for sulphur (signal S 2p) was performed applying an area-ratio-constraint of 2:1 for the two components of the signal ($p_{3/2}$ and $p_{1/2}$), in accordance with spin-orbit splitting [40]. Also, a position-difference-constraint of 1.25 eV is applied for the two components of the sulphur signal. In order to inspect the elemental contribution of the tribofilm throughout its depth, Ar^+ ion source (2 keV energy, 2 ×2 mm^2 area, and 1 µA sputter current) has been used to sputter the tribofilm. Ion sputtering was carried out every 60 s between XPS acquisition.

3.3 Surface and tribofilm inspection in nano-metre scale using TEM and EDX

A cross section of the worn area on the roller surface after a million load cycles was prepared by FIB using a FEI Nova 200 NanoLab high resolution Field Emission Gun Scanning Electron Microscope (FEG-SEM). FIB lamella is collected from an area close to the edge of a micropit perpendicular to the rolling/sliding direction and examined using TEM. TEM images were obtained utilising a FEI Tecnai TF20 FEG-TEM/STEM. EDX analysis was employed to identify tribofilm elements within the film. An Oxford Instruments INCA 350 EDX system equipped with X-Max SDD detector and Gatan Orius SC600A CCD camera was used to produce elemental mapping. The thickness of the prepared lamella is less than 100 nm also the beam energy is much greater than that of SEM, as a result the interaction volume of the electron beam with the specimen is negligible compared to EDX-SEM which brings about less beam scattering and a consequent significantly higher spatial resolution compared to SEM[41].

4 Results and discussion

4.1 Imaging surface fatigue features

Figure 2(a) shows the SEM image of the roller surface with the tribofilm on top, which exhibits cracking of the roller surface and the reaction layer. Following removal of the tribofilm micropits can be clearly observed in **Figure 2**(b and c). The micropitting on the surface indicates an occurrence of a severe surface fatigue on the roller surface. At a higher magnification, shown in **Figure 2**(d), appearance of micropits elucidates its propagate opposite to the sliding direction into the bulk of the material and also transverse to the rolling/sliding direction [42].

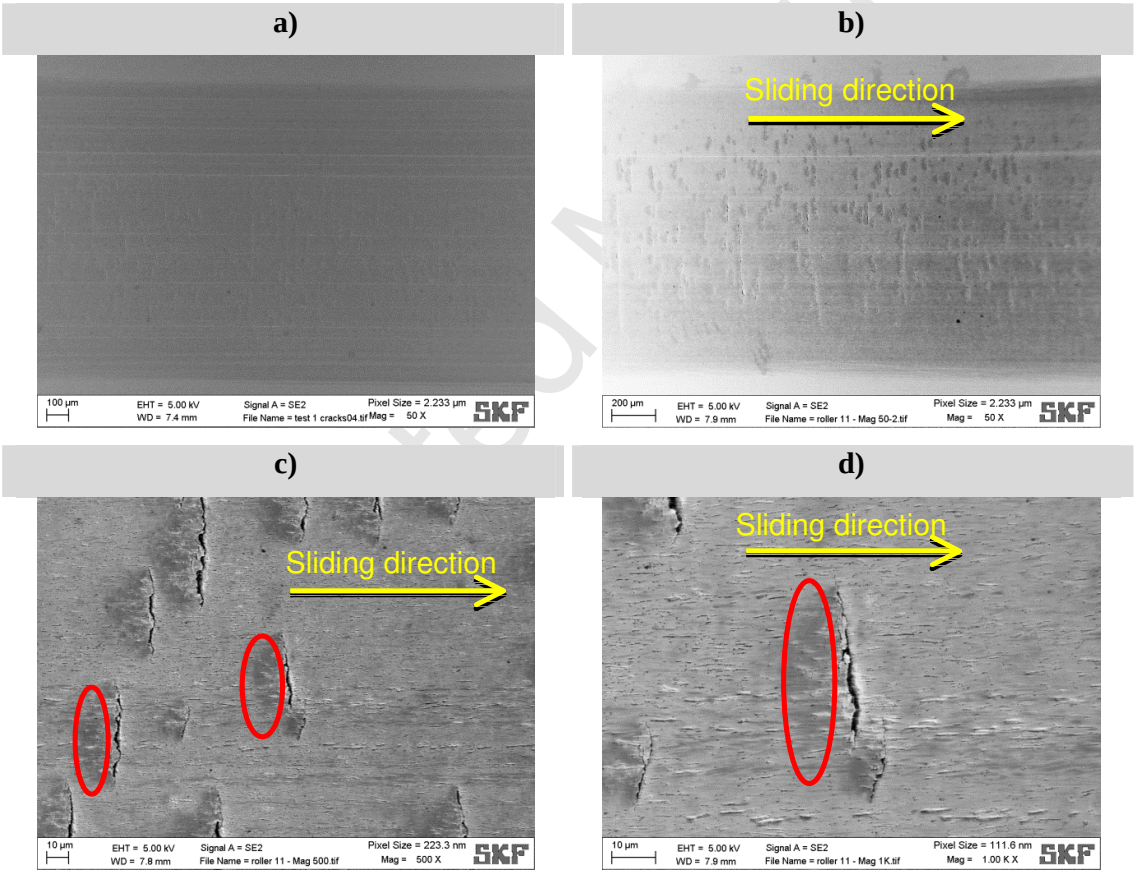

Figure 2. SEM images of the roller surface a) with reaction layer on the surface, b, c, d) after washing procedure

Associated with each induvial micropit, a dark region is visible in **Figure 2** (c & d) surrounding the micropits which is annotated on the images using an ellipse. Image contrast in the SE mode of SEM is particularly governed by edge effect which represents the surface topographical characteristics. The darker regions are the zones with a lower electron escape

and represent rougher surface which can be an indication of a chemical etching induced by enhanced local-reactivity of ZDDP under severe contacts. A dramatically intensified reactivity of additive on the surface has been postulated to act as a pit nuclei [6].

4.2 Chemical investigation of tribofilm in micro-scale

In **Figure 3**(a) the survey spectra collected from the very top surface (denoted as survey spectrum) and from surface after etching the tribofilm for 540 s using Ar^+ ion sputtering (denoted as survey after etching) are shown. No peak was detected in the detailed signals of the tribofilm elements (P, S, Zn) after 600 s of ion sputtering. Therefore, 540 seconds of ion sputtering is considered as the last step of the etching at which the tribofilm elements are detected. Associated detailed signals of the tribofilm elements (P, S, Zn) after 540 s of ion sputtering are shown in **Figure 3**(b, c and d) and denoted as detailed spectra after etching. All the ZDDP tribofilm elements are detected in the detailed spectra after etching implying that a distinct layer of Fe/Zn sulphide does not exist at the interface between phosphate and steel.

The detailed signals of sulphur and carbon collected from the very top surface and the surface after etching are shown in **Figure 4**(a and b).The S signal has a $2p_{3/2}$ peak at binding energy of 162.4 ± 0.1 eV and 161.8 ± 0.2 eV in the signal collected from the very top surface and the signal after etching the tribofilm, respectively. A binding energy close to 162 eV in sulphur signal corresponds to an oxidation state of -2 (Sll) and is assigned to sulphides [43]. The contribution of the sulphide to the top layer of the tribofilm is attributed to metal sulphide (ZnS here), organic sulphides and sulphur which is substituted for the oxygen in the phosphate chain forming (polythio)phosphate (O-P-O → O-P-S) [20, 22].

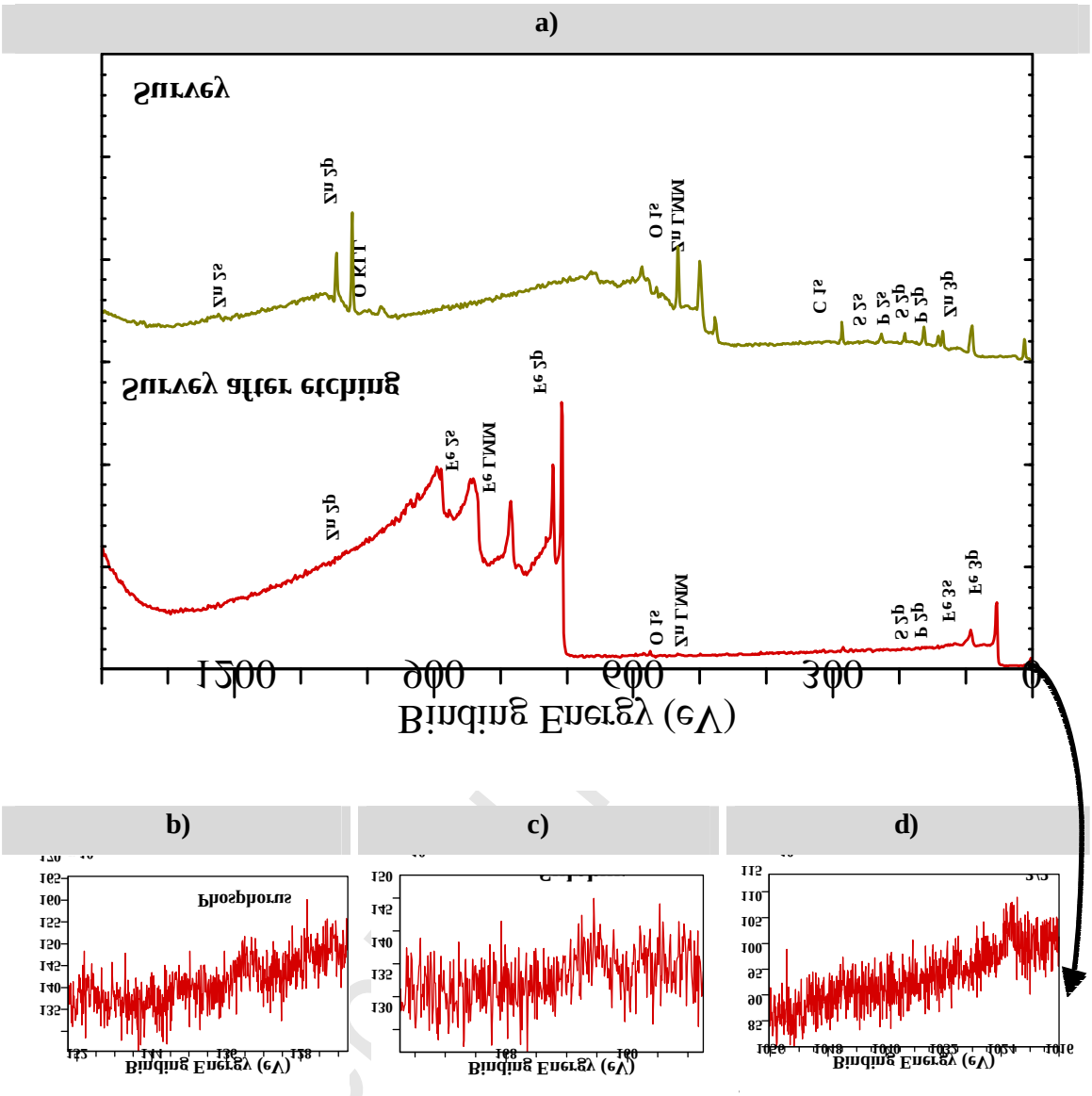

Figure 3. a) Survey spectra collected from the wear scar and corresponding b) phosphorous c) sulphur and c) zinc detailed spectra after etching

The zinc modified Auger parameter (α'= Zn $2p_{3/2}$ (BE) + Zn $L_3M_{4,5}M_{4,5}$ ^1G (KE)) is calculated to be 2010.2 ± 0.2 eV at the top surface which indicates that most of the zinc is present as zinc oxide rather than zinc sulphide [42]. This shows that zinc mostly contributes to the tribofilm through zinc phosphate formation in agreement with the previous reports [21, 23, 39]. The carbon signal obtained from the tribofilm after etching is arising from carbide and specifies the principally inorganic nature of the tribofilm. Thus, the sulphide signal collected from the surface after etching the tribofilm is attributed to metal sulphides (ZnS or Fe_xS_y). The Fe $2p_{3/2}$ signal after etching the tribofilm is resolved to two peaks; the first peak

appeared at 706.6 ± 0.1 eV which corresponds to metallic iron and the second peak appears at 710.5 ± 0.1 eV. The contribution of the second peak is minor (4.5% of the total Fe $2p_{3/2}$ signal) and can be predominantly attributed to the iron oxide and/or iron phosphate.

The O 1s signal after etching the tribofilm consists of two peaks at 530.3 ± 0.1 eV and 531.7 ± 0.1 eV. The first peak can be attributed to metal-oxides particularly ZnO rather than iron oxide since iron oxide mainly appears at lower binding energies (close to 529.8 eV) compared to ZnO. Moreover, iron oxide at the ZDDP tribofilm-substrate interface is not expected to endure within the contact according to the HSAB model [20, 22] and prevailing experimental results from Minfray et al. [30, 39]. The second peak at 531.7± 0.1 eV, assigned to non-bridging oxygen [22], corresponds to oxygen in the phosphate chain (-P=O and P-O-

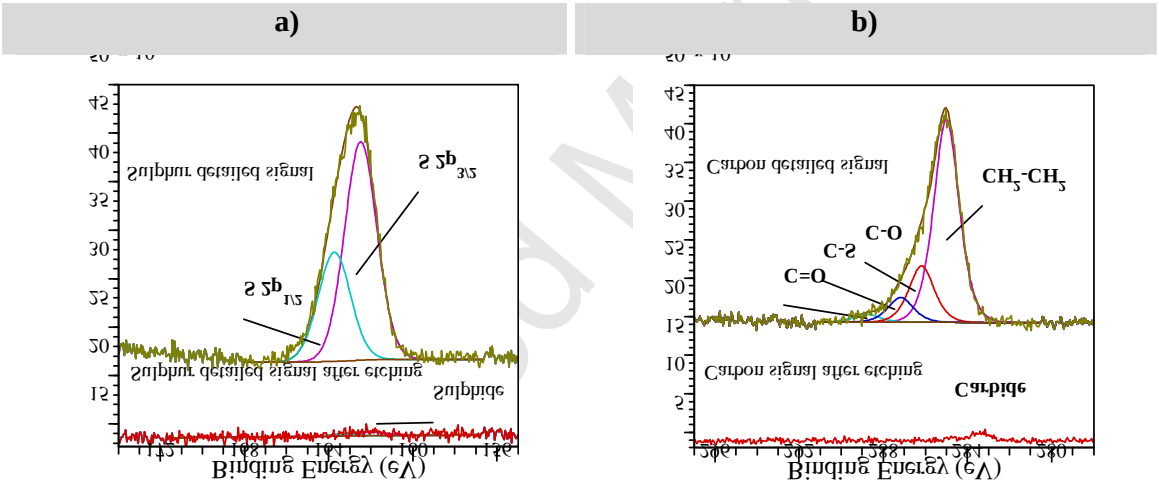

Figure 4. a) Sulphur and b) carbon detailed spectra on the very top surface and after etching M; where M is metal: Fe/Zn) and hydroxides [40, 42].

In accordance with of the XPS results, a mixed Zn/Fe phosphates and zinc sulphide/oxide can be suggested as the composition of the tribofilm after etching lacking a distinct layer of Fe/Zn oxide/sulphide. Although the XPS Ar^+ ion sputtering is a useful technique in order to inspect the tribofilm elemental distribution through its depth, compounds could be affected through preferential sputtering and intermixing the compounds [44] especially in the case of transition metals. In the case of iron, iron oxides can undergo reduction to other oxidation states [45, 46]. Therefore, loss of analysis resolution is expected through depth profiling.

4.3 Surface and tribofilm inspection at the nano-metre scale: imaging and elemental-mapping of the reaction layer

4.3.1 Iron sulphide formation on interface

Figure 5 shows the ZDDP tribofilm formed on the surface which is in agreement with our XPS data and previous reports [17, 22]. As shown in **Figure 5** (Zn K-line), zinc exists extensively on the top layer while declines in concentration towards the bulk of the tribofilm. A small contribution of iron to the tribofilm can be detected in the bottom 30 nm of the tribofilm. **Table 2** (a and b) compares the distribution of the tribofilm elements in top and middle layers of the tribofilm. The atomic concentration ratio of oxygen to phosphorous is similar in the both layers. In contrast to that, atomic concentration ratio of sulphur and zinc to phosphorous is decreased at mid-layer, suggesting less contribution of the sulphide to the tribofilm bulk.

In **Figure 5** (S K-line) two distinct areas can be discerned in which presence of sulphur is more pronounced; the very top layer and very bottom layer. Elemental EDX mapping of iron and sulphur presents the merged mapping of the iron and sulphur. At the very bottom layer of the tribofilm where sulphur concentration is intensified, solely detected elements are sulphur and iron. Considering the XPS data (**Figure 4(**a)) showing an entirely sulphide contribution from sulphur signal, a distinct and interfacial 5-10 nm iron sulphide layer formation is confirmed at the substrate of the steel. In agreement with Martin et al. [22] and Minfray et al. [30, 39, 47] no iron oxide layer is observed at the interface according to XPS and TEM-EDX mapping results.

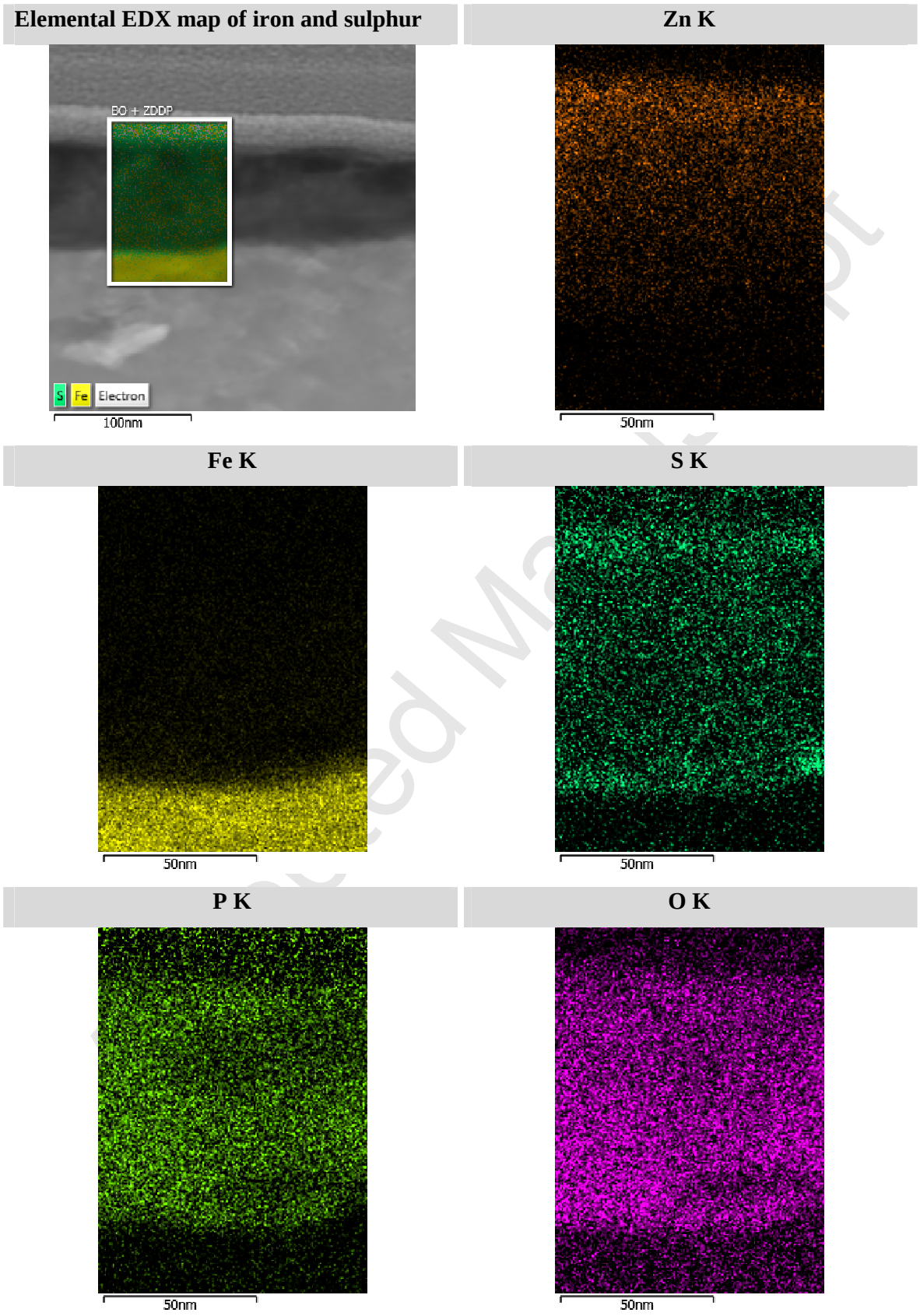

Figure 5. EDX elemental mapping of the tribofilm from FIB sample

Figure 6 (S K-line) exhibits an area of the lamella in which a crack has been initiated. Once again, two distinct lines confirm the greater presence of sulphur on the very top-layer and very bottom-layer of the tribofilm which are more conspicuous in comparison to **Figure 5**. Also, the EDX merged mapping of iron and sulphur clearly indicates the formed iron sulphide interfacial layer at the substrate. Interestingly the elemental distribution of the tribofilm in the area in which a crack is initiated (**Figure 6**) is different from other part of the FIB sample in which no crack was observed (**Figure 5**). In contrast to **Figure 5**, zinc greatly contributes to the bulk of the tribofilm, probably mostly as zinc (poly) phosphate together with zinc sulphide. A punctilious consideration of the oxygen and phosphorous maps asserts that oxygen and phosphorous coexist at the same areas of the maps corresponding to phosphates. Furthermore, in the tribofilm bulk, above the iron-sulphide interfacial layer, sulphur and zinc signals enhanced at a same area inferring an increased zinc sulphide contribution to the tribofilm bulk associated with the cracked surface. The enhanced sulphide formation on the substrate and in the tribofilm bulk states an escalated sulfur (re)activity close the cracked site.

Comparing **Figure 5** and **Figure 6**, it is clear that the tribofilm unevenly distributed on the surface of the roller and the thickness of the tribofilm varies from 20 nm to 100 nm. Thickness variation is probably due to the uneven wear on the surface resulted from localised surface damage. The elemental demonstration of the tribofilm, shown in **Figure 5**, is in agreement with the literature [17] and our XPS results; while **Figure 6** demonstrates an altered compound distribution in the tribofilm near to the crack initiated site at which iron sulphide formation is enhanced. This suggests that XPS data is influenced by the averaging effect over the analysed area. In addition, XPS depth profiling could not detect a distinct layer on the interface implying a localised formation of the iron sulphide near the micropit verifying previous studies [6, 48] which suggest localised enrichment of sulfur traces around the pits.

Table 2. EDX spectra and atomic concentration ratio of the tribofilm elements at a) top layer b) middle layer

a)

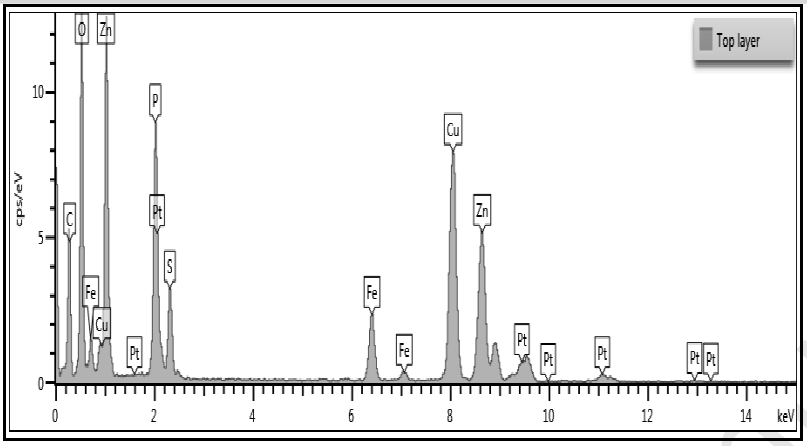

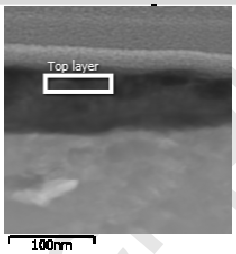

Atomic concentration ratio

Zn/P: 0.7

S/P: 0.4

O/P: 3.8

b)

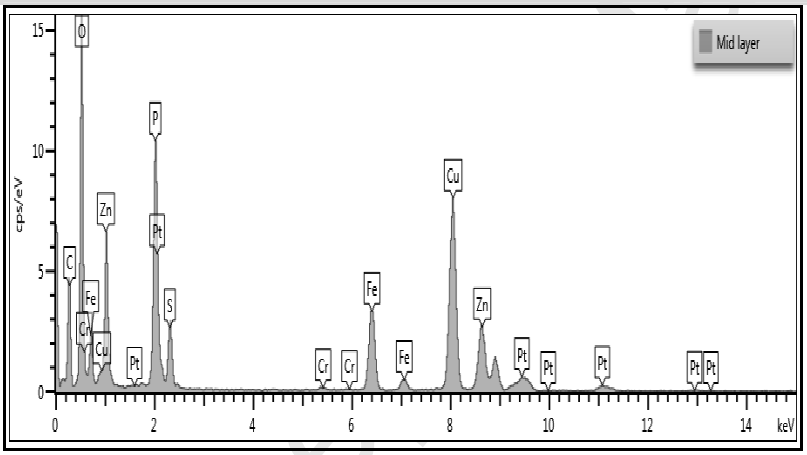

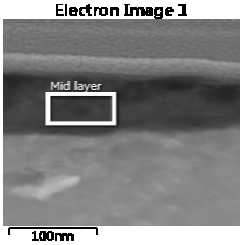

Atomic concentration ratio

Zn/P: 0.3

S/P: 0.3

O/P: 3.8

4.3.2 Effect of the lubricant additive on surface cracks

Alongside the iron sulphide formation induced by the interaction of the ZDDP elements and steel substrate, lubricant additives can interact with surface initiated cracks [6, 49]. Lubricants can enter the crack leading to an accelerated fatigue crack propagation by reducing the friction acting between the crack faces [50] or by exerting hydraulic pressure on the crack faces [50, 51]. The ingress of large amount of oxygen and carbon into the microcracks has been observed in a tapered roller bearing lubricated with base oil [52]. Alongside base oil, additives also penetrate into the microcracks. Additive interaction with the crack faces has also been shown previously [49, 53, 54]. However, key understanding of

this interaction with regards to reaction kinetics and chemical composition of the compounds derived from the interaction is missing. Also, the effect of additive traces inside the microcracks on the crack propagation is arguable. Evans et al. [55] have not observed corrosive attack of sulphur- and phosphorus-containing additives to the surface, unless the extreme pressure additive is highly active [56]. On the other hand, several reports [5-7, 9, 57] evidence reduced fatigue life associated with enhanced chemical attack of additives.

Elemental EDX merged mapping of iron and sulphur

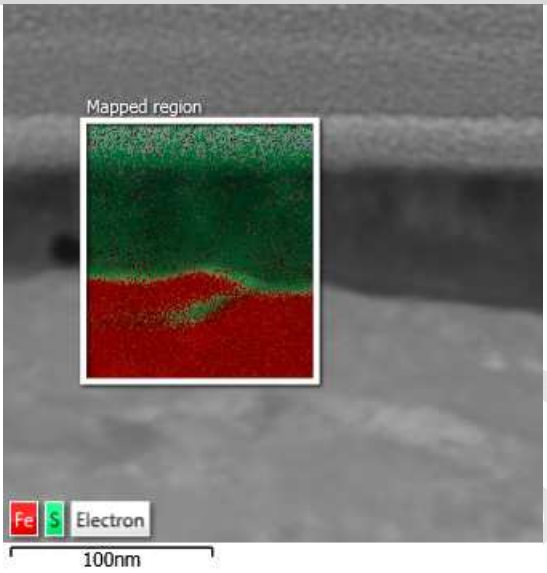

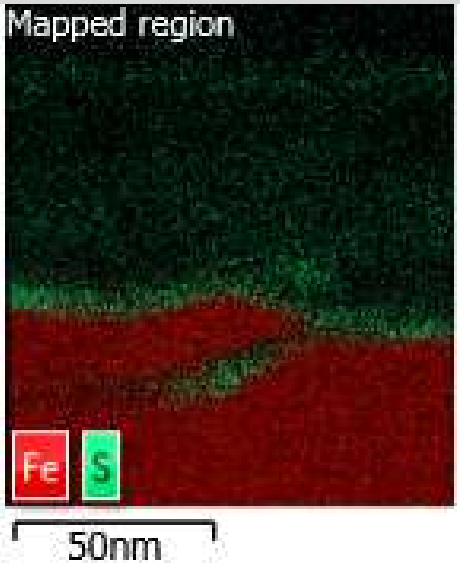

Fe K | **S K**

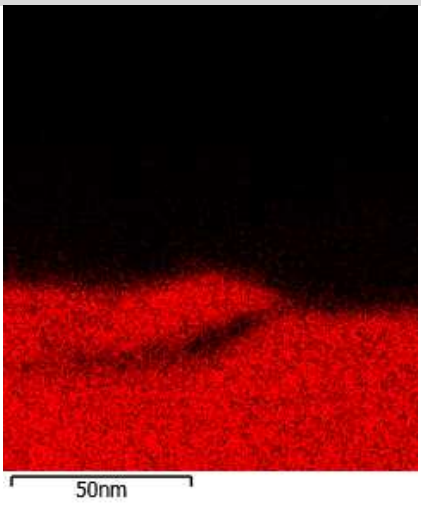

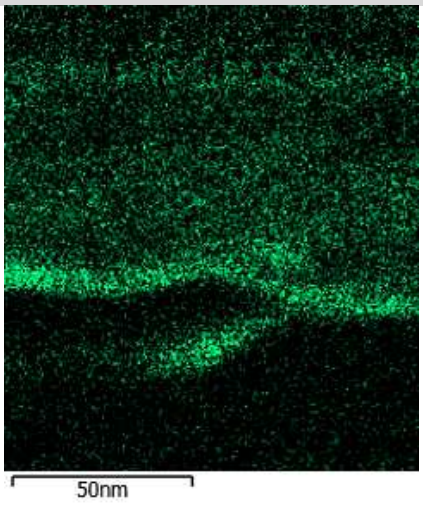

P K | **Zn K**

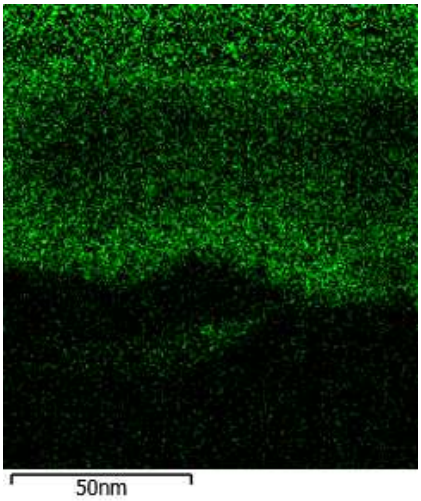

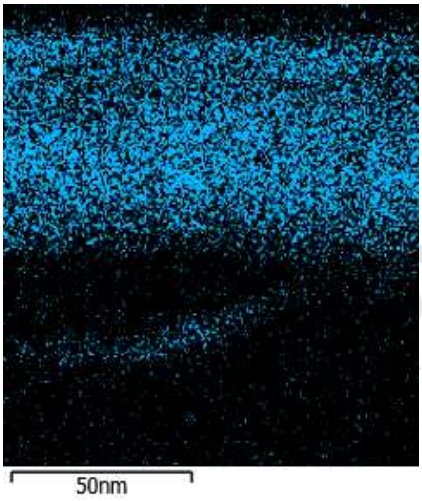

Fe and P merged-mapping	Fe and Zn merged-mapping

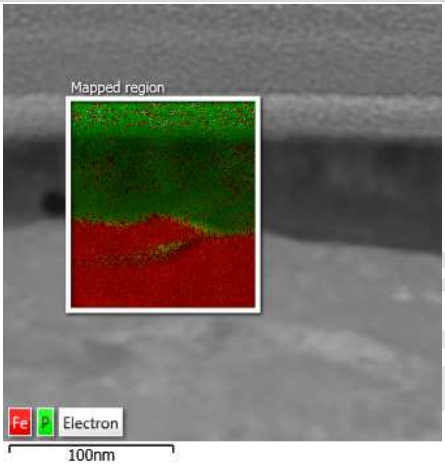

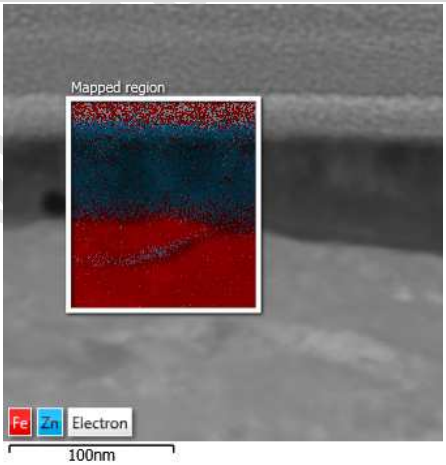

O K	Fe and O merged-mapping

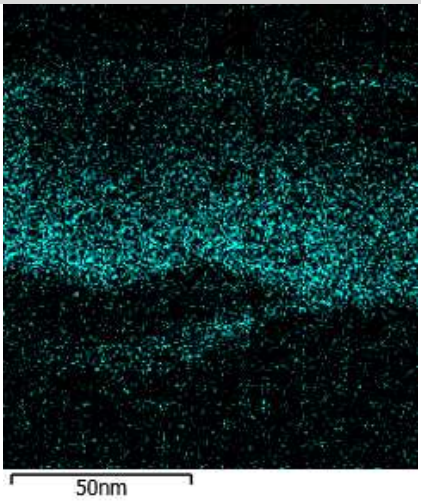

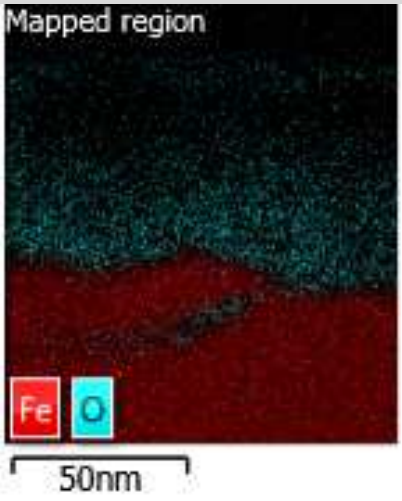

Figure 6. EDX elemental mapping of the tribofilm from FIB sample in the cracked zone

The ingress of the ZDDP elements into the crack can be clearly observed in **Figure 6** which presents a surface initiated crack. **Table 3** specifies the atomic concentration ratio of the ZDDP elements inside the crack at different crack zones. Considering the ratios presented in **Table 2**, an enormous contribution of sulphur species is observed inside the crack. The atomic concentration ratio of sulphur to phosphorous in the top layer of the tribofilm is 0.6 as an average (according to the XPS results) and 0.3 in the bulk of the tribofilm. However, inside the crack the ratio is always larger than 1, reaching 2.9 at the crack-mouth which is greater than the ratio in ZDDP molecule ($\frac{S(at\%)}{P(at\%)} = 2$). The atomic concentration of the phosphorous and zinc at the mid-crack and crack-tip remained similar while no zinc was detected at the crack-mouth. In contrast to phosphorous and zinc, sulphur atomic concentration is higher at crack-mouth and decreases towards the crack-tip. In agreement with the presented results in **Table 3**, an enhanced sulphur concentration inside a crack, induced by rolling-sliding contacts, is observed by Meheux et al. [49].

The affinity of the additive to interact with the crack faces and form a compound inside the crack can also be addressed through electronic state of the molecules. At the crack tips where increase in interatomic distance is large, due to the change in the Morse potential, activation energy of the reaction is decreased. Reduction in the required activation energy, favours the reaction of the additive elements with the crack tip [18]. As shown the concentration of sulphur is high inside the crack favouring formation of iron-sulphur compounds.

Iron sulphide in the presence of oxygen can be oxidised to other types of iron sulphide [58] or magnetite iron oxide [27]. While oxidation of the iron sulphide at high temperatures (around 500°C) can produce magnetite or iron oxide (which can occur in the flash temperatures happening in the asperity contacts), oxidation at the lower temperatures can lead to the conversion of iron sulphide to the other types of iron sulphides.

Potentially detrimental influence of the chemical interaction of the additive with the microcracks can be considered as stress corrosion cracking (SCC) induced by penetrated oil and additives [18, 59], which can reduce the self-healing ability of the crack [53] and accelerate crack propagation in the presence of small amount of water and oxygen [59]. Since iron sulphide is electro conductive, localised formation of the iron sulphide around the pit or crack, can induce localised electrolytic corrosion inside the pit (iron as an anode) in the presence of electrolyte (water) forming a local electrochemical cell [58]. In other words, iron

sulphide in the presence of water and oxygen depending on the pH of the local environment can react to generate iron hydroxide+ sulphuric acid or ferrous iron + sulphate + acidity [60]. Sulphate and acidic reaction products can enhance SCC. Water ingress into the crack can be expected by considering capillary crack condensation (CCC) hypothesis [61]. The CCC suggests that small amount of dissolved water can induce significant amount of condensed water inside the microcracks [61]. These phenomena can be addressed as stress corrosion crack propagation effect of the additive elements especially sulphur. Moreover, presence of additive elements inside the crack as tribofilm, may reduce the friction coefficient between crack faces [62] and supress adhesion of the crack faces under rolling contact which results in accelerated crack propagation [50]. In agreement with the results in this study, enhanced existence of the sulphur at the crack tip was observed for the lubricant formulations with shorter fatigue lives [49, 62] which supports SCC effect of sulphur on the microcracks.

Table 3. Atomic concentration ratio of the ZDDP elements at the a) crack mouth b) middle of the crack c) crack tip

		a)	b)	c)
		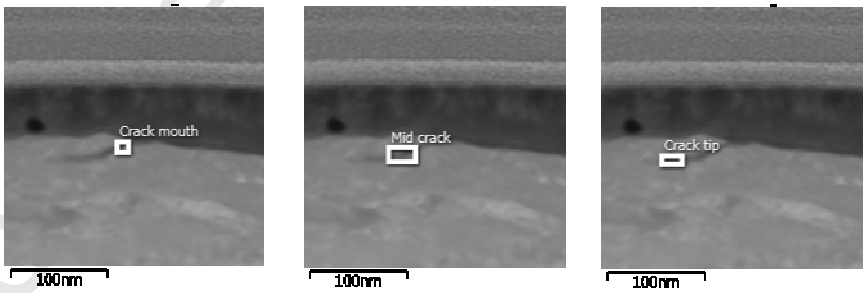		
Atomic concentration ratio	Zn/P	0	0.5	0.7
	S/P	2.9	2.1	1.1

In contrast to the SCC negative influence of the additive interaction with the microcracks, it is suggested that formation of the tribofilm earlier than crack initiation can act as sticking plaster which mitigates crack propagation [49]. Furthermore, if traces of ZDDP elements

inside the crack is recognised as tribofilm [62], CCC can be mitigated leading to an alleviated SCC effect. However, the effect of water on ZDDP tribofilm removal [40, 42] and hydrolysis [63, 64] should also be acknowledged. In other words, if water in lubricant is considerable enough to remove the tribofilm, the SCC can be intensified as a result of reactive sulphur species regardless of ascribing the additive elements inside the crack to an additive-derived film or traces of additive decomposition products.

As far as micropitting is concerned, Laine et al. [10] attributed the enhancing properties of ZDDP to its preventive effect on proper running-in wear of the rough surfaces. However, considering solely the additive influence on running-in, cannot entirely justify the O'Connor's [13] results showing that micropitting performance significantly depends on the chemical structure of the additives. The findings in this study shows an upsurge of sulphur reactivity and its localised attack under severe conditions leading to an intensified iron sulphide formation and subsequent sulphur ingress into the crack. The interaction of the sulphur with the crack faces and tip can induce stress corrosion cracking and accelerated fatigue crack growth. Thus, sulphur and steel interactions which is capable of protecting the surface from scuffing and abrasive wear, can facilitate surface fatigue initiation and propagation under certain circumstances. Therefore, substantial role of enhanced chemical attack of the additive-derived compounds especially sulphur species in micropitting-enhancing behaviour of ZDDP should be put forward alongside attributing the behaviour of ZDDP to its tendency to impede lubricant entrainment [65], chemically modified tribofilm in the severe contact [12] and delaying effect on running-in [10].

5 Conclusions

In the current study the tribochemical interaction of ZDDP with the steel surface under severe micropitting wear has been studied. A 5-10 nm thin iron sulphide layer is visualised on the interface as a separate layer underneath the phosphate layer with an altered distribution of tribofilm elements near the crack site. Iron sulphide reaction layer is localised on the surface of steel and enriched with higher concentration of sulphur near the cracked site implying greater EP activity of ZDDP near the crack site. Following removal of the tribofilm, grey reaction layer was observed on the wear track preferentially surrounding the micropits which may correspond to sulphur attack to the surface and locally enhanced formation of iron-sulphur compounds.

Elemental mapping of the tribofilm generated from ZDDP showed the heterogeneous nature of the tribofilm throughout its depth and more interestingly from one site to the other site of the FIB lamella. Distribution of the ZDDP tribofilm elements in the tribofilm near a crack-initiated site is different from a substrate site without crack.

ZDDP additive elements have been observed inside the crack with the enhanced contribution of the sulphur. The ZDDP elemental distribution inside the crack is different from crack mouth to crack tip. The potential influence of the additive attack to the surface and crack faces and tip has been discussed considering the current existing literature. While iron sulphide formation can mitigate scuffing and abrasive wear, presence of the ZDDP traces inside the initiated cracks may induce stress corrosion crack propagation especially in a bearing which operates in a tribocorrosive environment where water is diffused into the lubricant.

6 Acknowledgments

This study was funded by the FP7 program through the Marie Curie Initial Training Network (MC-ITN) entitled "FUTURE-BET-Formulating an Understanding of Tribocorrosion in ArdUous Real Environments – Bearing Emerging Technologies" (317334) and was carried out at University of Leeds and SKF Engineering and Research Centre. The authors would like to thank to all FUTURE-BET partners whom had kind discussions on the topic and the methodology.

7 References:

[1] X. Wu, J. Zhang, W. Qi, X. Gu, L. Zhang, The effect of SP gear oil on load capacity of carburized gears, in: P. MCI, FRANCE (1999) (Ed.) 4th World congress on gearing and power transmission Paris, France, 1999.
[2] H.S. Hong, M. Huston, B. O'Connor, N. Stadnyk, Evaluation of surface fatigue performance of gear oils, Lubr. Sci., 10 (1998) 365-380.
[3] W. Tuszynski, An effect of lubricating additives on tribochemical phenomena in a rolling steel four-ball contact, Tribol. Lett., 24 (2006) 207-215.
[4] H.K. Trivedi, N.H. Forster, L. Rosado, Rolling contact fatigue evaluation of advanced bearing steels with and without the oil anti-wear additive tricresyl phosphate, Tribol. Lett., 41 (2011) 597-605.
[5] G. Wan, E. Amerongen, H. Lankamp, Effect of extreme-pressure additives on fatigue life of rolling bearings, J. Phys. D: Appl. Phys., 25 (1992) 147-153.
[6] A. Torrance, J. Morgan, G. Wan, An additive's influence on the pitting and wear of ball bearing steel, Wear, 192 (1996) 66-73.
[7] H.P. Nixon, H. Zantopulos, Lubricant additives, friend or foe. What the equipment design engineer needs to know, Lubr. Eng., 51 (1995) 815-822.

[8] H. Pasaribu, P. Lugt, The composition of reaction layers on rolling bearings lubricated with gear oils and its correlation with rolling bearing performance, Tribol. Trans., 55 (2012) 351-356.
[9] A. Torrance, Chemical and microstructural changes induced in bearing steel by rolling contact, Wear, 122 (1988) 363-376.
[10] E. Lainé, A.V. Olver, M.F. Lekstrom, B.A. Shollock, T.A. Beveridge, D.Y. Hua, The effect of a friction modifier additive on micropitting, Tribol. Trans., 52 (2009) 526-533.
[11] P. Brechot, A. Cardis, W. Murphy, J. Theissen, Micropitting resistant industrial gear oils with balanced performance, Ind. Lubr. Tribol., 52 (2000) 125-136.
[12] S. Soltanahmadi, A. Morina, M.C. van Eijk, I. Nedelcu, A. Neville, Investigation of the effect of a diamine-based friction modifier on micropitting and the properties of tribofilms in rolling-sliding contacts, Journal of Physics D: Applied Physics, 49 (2016) 505302.
[13] B. O'connor, The influence of additive chemistry on micropitting, Gear Technology, 22 (2005) 34-41.
[14] H. Spikes, A. Olver, P. Macpherson, Wear in rolling contacts, Wear, 112 (1986) 121-144.
[15] A. Oila, S. Bull, Assessment of the factors influencing micropitting in rolling/sliding contacts, Wear, 258 (2005) 1510-1524.
[16] K. Allum, E. Forbes, The load-carrying properties of metal dialkyl dithiophosphates: the effect of chemical structure, in: Proceedings of the Institution of Mechanical Engineers, Conference Proceedings, SAGE Publications, 1968, pp. 7-14.
[17] H. Spikes, The history and mechanisms of ZDDP, Tribol. Lett., 17 (2004) 469-489.
[18] T. Fischer, Tribochemistry, Annual Review of Materials Science, 18 (1988) 303-323.
[19] M. Najman, M. Kasrai, G. Bancroft, X-ray absorption spectroscopy and atomic force microscopy of films generated from organosulfur extreme-pressure (EP) oil additives, Tribol. Lett., 14 (2003) 225-235.
[20] J.M. Martin, Antiwear mechanisms of zinc dithiophosphate: a chemical hardness approach, Tribol. Lett., 6 (1999) 1-8.
[21] M. Kasrai, M.S. Fuller, G.M. Bancroft, E.S. Yamaguchi, P.R. Ryason, X-ray absorption study of the effect of calcium sulfonate on antiwear film formation generated from neutral and basic Zddps: Part 2—sulfur species, Tribol. Trans., 46 (2003) 543-549.
[22] J.M. Martin, C. Grossiord, T. Le Mogne, S. Bec, A. Tonck, The two-layer structure of Zndtp tribofilms: Part I: AES, XPS and XANES analyses, Tribol. Int., 34 (2001) 523-530.
[23] Z. Zhang, E. Yamaguchi, M. Kasrai, G. Bancroft, X. Liu, M. Fleet, Tribofilms generated from ZDDP and DDP on steel surfaces: Part 2, chemistry, Tribol. Lett., 19 (2005) 221-229.
[24] R. Mourhatch, P.B. Aswath, Tribological behavior and nature of tribofilms generated from fluorinated ZDDP in comparison to ZDDP under extreme pressure conditions—Part 1: Structure and chemistry of tribofilms, Tribol. Int., 44 (2011) 187-200.
[25] M. De Barros, J. Bouchet, I. Raoult, T. Le Mogne, J. Martin, M. Kasrai, Y. Yamada, Friction reduction by metal sulfides in boundary lubrication studied by XPS and XANES analyses, Wear, 254 (2003) 863-870.

[26] M. Hallouis, M. Belin, J. Martin, The role of sulphur in ZDDP-induced reaction films formed in the presence of ZDDP: Contribution of electron spectroscopic imaging technique, Lubr. Sci., 2 (1990) 337-349.
[27] M. Watanabe, M. Sakuma, T. Inaba, Y. Iguchi, Formation and oxidation of sulfides on pure iron and iron oxides, Materials transactions-JIM, 41 (2000) 865-872.
[28] S. Jahanmir, Wear reduction and surface layer formation by a ZDDP additive, J. Tribol., 109 (1987) 577-586.
[29] W. Glaeser, D. Baer, M. Engelhardt, In situ wear experiments in the scanning Auger spectrometer, Wear, 162 (1993) 132-138.
[30] C. Minfray, T. Le Mogne, A. Lubrecht, J.-M. Martin, Experimental simulation of chemical reactions between ZDDP tribofilms and steel surfaces during friction processes, Tribol. Lett., 21 (2006) 65-76.
[31] J. Bell, K. Delargy, A. Seeney, Paper IX (ii) The Removal of Substrate Material through Thick Zinc Dithiophosphate Anti-Wear Films, Tribology series, 21 (1992) 387-396.
[32] G. Smith, J. Bell, Multi-technique surface analytical studies of automotive anti-wear films, Applied surface science, 144 (1999) 222-227.
[33] Z. Yin, M. Kasrai, M. Fuller, G.M. Bancroft, K. Fyfe, K.H. Tan, Application of soft X-ray absorption spectroscopy in chemical characterization of antiwear films generated by ZDDP Part I: the effects of physical parameters, Wear, 202 (1997) 172-191.
[34] M. Najman, M. Kasrai, G. Bancroft, Chemistry of antiwear films from ashless thiophosphate oil additives, Tribol. Lett., 17 (2004) 217-229.
[35] Z. Yin, M. Kasrai, G.M. Bancroft, K.F. Laycock, K.H. Tan, Chemical characterization of antiwear films generated on steel by zinc dialkyl dithiophosphate using X-ray absorption spectroscopy, Tribol. Int., 26 (1993) 383-388.
[36] Z. Zhang, E. Yamaguchi, M. Kasrai, G. Bancroft, Tribofilms generated from ZDDP and DDP on steel surfaces: Part 1, growth, wear and morphology, Tribol. Lett., 19 (2005) 211-220.
[37] G. Pereira, D. Munoz-Paniagua, A. Lachenwitzer, M. Kasrai, P.R. Norton, T.W. Capehart, T.A. Perry, Y.-T. Cheng, A variable temperature mechanical analysis of ZDDP-derived antiwear films formed on 52100 steel, Wear, 262 (2007) 461-470.
[38] B. Kim, R. Mourhatch, P.B. Aswath, Properties of tribofilms formed with ashless dithiophosphate and zinc dialkyl dithiophosphate under extreme pressure conditions, Wear, 268 (2010) 579-591.
[39] C. Minfray, J. Martin, C. Esnouf, T. Le Mogne, R. Kersting, B. Hagenhoff, A multi-technique approach of tribofilm characterisation, Thin Solid Films, 447 (2004) 272-277.
[40] I. Nedelcu, E. Piras, A. Rossi, H. Pasaribu, XPS analysis on the influence of water on the evolution of zinc dialkyldithiophosphate–derived reaction layer in lubricated rolling contacts, Surface and Interface Analysis, 44 (2012) 1219-1224.
[41] D.B. Williams, C.B. Carter, The transmission electron microscope, Springer, 1996.
[42] S. Soltanahmadi, A. Morina, M.C.P. van Eijk, I. Nedelcu, A. Neville, Tribochemical study of micropitting in tribocorrosive lubricated contacts: The influence of water and relative humidity, Tribol. Int., 107 (2017) 184-198.

[43] D. Brion, Etude par spectroscopie de photoelectrons de la degradation superficielle de FeS 2, CuFeS 2, ZnS et PbS a l'air et dans l'eau, Applications of Surface Science, 5 (1980) 133-152.
[44] C. Wagner, D. Briggs, M. Seah, Practical surface analysis, Auger and X-ray Photoelectron Spectroscopy, 1 (1990) 595.
[45] E. Paparazzo, XPS analysis of iron aluminum oxide systems, Applied surface science, 25 (1986) 1-12.
[46] P. Mills, J. Sullivan, A study of the core level electrons in iron and its three oxides by means of X-ray photoelectron spectroscopy, Journal of Physics D: Applied Physics, 16 (1983) 723.
[47] C. Minfray, J.-M. Martin, M. De Barros, T. Le Mogne, R. Kersting, B. Hagenhoff, Chemistry of ZDDP tribofilm by ToF-SIMS, Tribol. Lett., 17 (2004) 351-357.
[48] T. Sakamoto, H. Uetz, J. Föhl, M. Khosrawi, The reaction layer formed on steel by additives based on sulphur and phosphorus compounds under conditions of boundary lubrication, Wear, 77 (1982) 139-157.
[49] M. Meheux, C. Minfray, F. Ville, T. Mogne, A. Lubrecht, J.-M. Martin, H.-P. Lieurade, G. Thoquenne, Effect of lubricant additives in rolling contact fatigue, Proceedings of the Institution of Mechanical Engineers, Part J: Journal of Engineering Tribology, 224 (2010) 947-955.
[50] A. Bower, The influence of crack face friction and trapped fluid on surface initiated rolling contact fatigue cracks, J. Tribol., 110 (1988) 704-711.
[51] M. Kaneta, Y. Murakami, Effects of oil hydraulic pressure on surface crack growth in rolling/sliding contact, Tribol. Int., 20 (1987) 210-217.
[52] R.D. Evans, K.L. More, C.V. Darragh, H.P. Nixon, Transmission electron microscopy of boundary-lubricated bearing surfaces. Part I: Mineral oil lubricant, Tribol. Trans., 47 (2004) 430-439.
[53] G. Galvin, H. Naylor, Effect of lubricants on the fatigue of steel and other metals, Proceedings of the Institution of Mechanical Engineers, 179 (1964) 857-875.
[54] P.U. Aldana, F. Dassenoy, B. Vacher, T. Le Mogne, B. Thiebaut, A. Bouffet, Anti spalling effect of WS2 nanoparticles on the lubrication of automotive gearboxes, Tribol. Trans., (2015) 00-00.
[55] R.D. Evans, K.L. More, C.V. Darragh, H.P. Nixon, Transmission electron microscopy of boundary-lubricated bearing surfaces. Part II: mineral oil Lubricant with sulfur-and phosphorus-containing gear oil additives, Tribol. Trans., 48 (2005) 299-307.
[56] R.D. Evans, H. Nixon, C.V. Darragh, J.Y. Howe, D.W. Coffey, Effects of extreme pressure additive chemistry on rolling element bearing surface durability, Tribol. Int., 40 (2007) 1649-1654.
[57] H.P. Nixon, Effects of extreme pressure additives in lubricants on bearing fatigue life, Iron and Steel Engineer, 75 (1998) 21-26.
[58] F.O. Pessu, Investigation of pitting corrosion of carbon steel in sweet and sour oilfield corrosion conditions: a parametric study, in, University of Leeds, 2015.
[59] S. Jahanmir, Examination of wear mechanisms in automotive camshafts, Wear, 108 (1986) 235-254.
[60] P.J. Sullivan, J.L. Yelton, K. Reddy, Iron sulfide oxidation and the chemistry of acid generation, Environmental Geology and Water Sciences, 11 (1988) 289-295.
[61] P. Schatzberg, I.M. Felsen, Effects of water and oxygen during rolling contact lubrication, Wear, 12 (1968) 331-342.

[62] V.C. Hostis BL, Minfray C, Frégonèse M, Jarnias F, Alder Da-Costa D'Ambros, Impact of lubricant formulation on pitting of manual transmission gears., In: 42nd Leeds-Lyon symposium on tribology, Lyon, France, 7-9 September 2015.
[63] H. Spedding, R. Watkins, The antiwear mechanism of zddp's. Part I, Tribol. Int., 15 (1982) 9-12.
[64] M.L.S. Fuller, M. Kasrai, G.M. Bancroft, K. Fyfe, K.H. Tan, Solution decomposition of zinc dialkyl dithiophosphate and its effect on antiwear and thermal film formation studied by X-ray absorption spectroscopy, Tribol. Int., 31 (1998) 627-644.
[65] L. Taylor, H. Spikes, Friction-enhancing properties of ZDDP antiwear additive: part I—friction and morphology of ZDDP reaction films, Tribol. Trans., 46 (2003) 303-309.

Keywords: Transmission Electron Microscopy (TEM); X-ray Photoelectron spectroscopy (XPS) surface analysis; Iron sulphide; Zinc Dialkyl DithioPhosphate (ZDDP); Micropitting

Highlights:

- A ZDDP-derived locally formed iron-sulphide layer is detected on the steel surface
- The iron-sulphide is a 5-10 nm thin distinct layer at steel-phosphate interface
- Near the surface-crack site the elemental distribution of the tribofilm is altered
- Sulphur concentration is enhanced in the iron-sulphide layer near the cracked-site
- ZDDP elements are detected inside the crack with a greater contribution of sulphur

Table of Contents/Abstract Graphic:

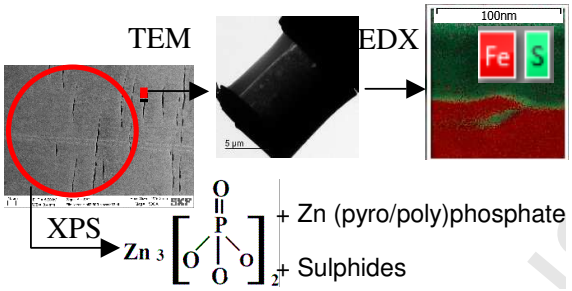

Chemical analysis of ZDDP-induced tribofilm under severe boundary lubricated regime in nano and micro-meter scales